Research Article

WCDMA Uplink Interference Assessment from Multiple High Altitude Platform Configurations

T. Hult,[1] D. Grace,[2] and A. Mohammed[1]

[1] *Department of Signal Processing, Blekinge Institute of Technology, 372 25 Ronneby, Sweden*
[2] *Department of Electronics, University of York, York, YO10 5DD, UK*

Correspondence should be addressed to T. Hult, tommy.hult@bth.se

We investigate the possibility of multiple high altitude platform (HAP) coverage of a common cell area using a wideband code division multiple access (WCDMA) system. In particular, we study the uplink system performance of the system. The results show that depending on the traffic demand and the type of service used, there is a possibility of deploying 3–6 HAPs covering the same cell area. The results also show the effect of cell radius on performance and the position of the multiple HAP base stations which give the worst performance.

1. INTRODUCTION

Third-generation mobile systems are gradually being deployed in many developed countries in hotspot areas. However, owing to the amount of new infrastructures required, it will still be some time before 3G is ubiquitous, especially in developing countries. One possible cost effective solution for deployments in these areas is to use high altitude platforms (HAPs) [1–9] for delivering 3G (WCDMA) communications services over a wide coverage area [10–14]. HAPs are either airships or planes that will operate in the stratosphere, 17–22 km above the ground. This unique position offers a significant link budget advantage compared with satellites and much wider coverage area than conventional terrestrial cellular systems. Such platforms will have a rapid rollout capability and the ability to serve a large number of users, using considerably less communications infrastructure than required by a terrestrial network [1]. In order to aid the eventual deployment of HAPs, the ITU has allocated spectrum in the 3G bands for HAPs [15], as well as in the mm-wave bands for broadband services at around 48 GHz worldwide [16] and 31/28 GHz for certain Asian countries [17].

Spectrum reuse is important in all wireless communications systems. Cellular solutions for HAPs have been examined in [18, 19], specifically addressing the antenna beam characteristics required to produce an efficient cellular structure on the ground, and the effect of antenna sidelobe levels on channel reuse plans [19]. HAPs will have relatively loose station-keeping characteristics compared with satellites, and the effects of platform drift on a cellular structure and the resulting intercell handover requirements have been investigated [20]. Cellular resource management strategies have also been developed for HAP use [21].

Configurations of multiple HAPs can also reuse the spectrum. They can be used to deliver contiguous coverage and must take into account coexistence requirements [11, 12]. A technique not widely known is their ability to serve the same coverage area reusing the spectrum to allow capacity enhancement. Such a technique has already been examined for TDMA/FDMA systems [22–24]. In order to achieve the required reduction in interference needed to permit spectrum reuse, the highly directional user antenna is used to spatially discriminate between the HAPs. The degree of bandwidth reuse and resulting capacity gain is dependent on several factors, in particular the number of platforms and the user antenna sidelobe levels.

In the case of many 3G systems, the user antenna is either omnidirectional or at best low gain, so in these cases it cannot be used to achieve the same effects. The purpose of this paper is to examine how the unique properties of a WCDMA system can be exploited in multiple HAP uplink architectures to deliver both coverage and capacity enhancements (without the need for the user antenna gain).

In addition to the spectral reuse benefits, there are three main benefits for a multiple HAP architecture as follows.

(i) The configuration also provides for incremental rollout: initially only one HAP needs to be deployed. As more capacity is required, further HAPs can be brought into service, with new users served by newly deployed HAPs.

(ii) Multiple operators can be served from individual HAPs, without the need for complicated coexistence criteria since the individual HAPs could reuse the same spectrum.

(iii) HAPs will be payload power, volume and weight constrained, limiting the overall capacity delivered by each platform. Capacity densities can be increased with more HAPs. Moreover, it may be more cost effective to use much lower capability HAPs [25] (e.g., solar powered planes), rather than one big HAP (e.g., solar powered airship), when covering a large number of cells.

The paper is organised as follows: in Section 2 the multiple HAP scenario is explained. The interference analysis is presented in Section 3. In Section 4, we examine the completely overlapping coverage area case, different numbers of platforms, and simulation results showing the achievable capacity enhancement are presented. Finally, conclusions are presented in Section 5.

2. MULTIPLE HAP SYSTEM SETUP

In this paper, we use a simple geometric positioning of the high altitude platforms to create signal environments that can easily be compared and analysed. In each constellation, the HAPs are located with equal separation along a circular contour, as shown in Figure 1.

The separation distance d_m along the line from the vertical projection of the HAP on the ground to the cell centre is varied from 70 km to zero (i.e., all the HAPs will be located on top of each other in the latter case).

All HAPs in this paper are assumed to be flying in the stratosphere at an altitude of 20 km. The size of the coverage area assigned to each HAP is governed by the shape of the base station antenna pattern. If we assume that we only have one cell per HAP, then the coverage area is also synonymous with the total cell area of the HAP.

2.1. User positioning geometry

Each user equipment (UE) is positioned inside the cell according to an independent uniform random distribution over the cell coverage area with radius R, as shown in Figure 2. The position of each UE inside each cell is defined relative to the HAP base station that it is connected to and also relative to every other HAP borne base station. This is necessary in order to evaluate the impact of interference between the different UE-HAP transmission paths.
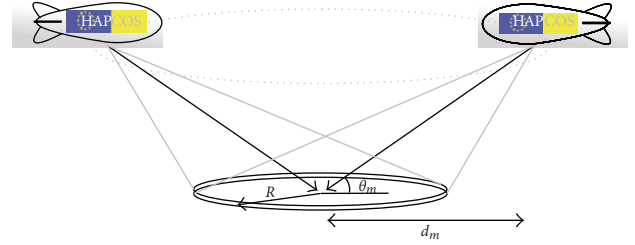

FIGURE 1: An example of a system simulation setup with $N = 2$ HAPs with overlapping cells of radius R. d_m is the distance on the ground between the cell centre and the vertical projection of the HAP on the ground and θ_m is the elevation angle towards the HAP.

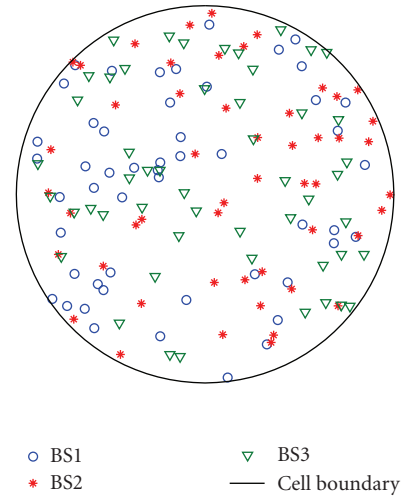| ○ | BS1 | ▽ | BS3 |
| * | BS2 | —— | Cell boundary |

FIGURE 2: A plot showing a sample distribution of 150 UE, where 50 UEs are assigned to each of the three base stations (BS1, BS2, and BS3).

2.2. Base station antenna pattern

The base station antenna pattern for the simulations was chosen to be simple but detailed enough to show the effects of the main and sidelobes, especially in the null directions, as illustrated in Figure 3. A simple rotationally symmetric pattern based on a Bessel function is used for this purpose, and is defined by [26]

$$G(\varphi) \approx 0.7 \cdot \left(\frac{2 \cdot J_1\left((70\pi/\varphi_{3\,\mathrm{dB}})\sin(\varphi)\right)}{\sin(\varphi)} \right)^2, \qquad (1)$$

where J_1 is a Bessel function of the first kind and order 1, $\varphi_{3\,\mathrm{dB}}$ is the 3 dB beam width in degrees of the main antenna lobe. The 3 dB beam width of the antenna is computed from the desired cell radius according to

$$\varphi_{3\,\mathrm{dB}} = 2 \cdot \mathrm{atan}\left(\frac{\mathrm{cellradius}}{\mathrm{HAP\ altitude}} \right). \qquad (2)$$

2.3. User equipment antenna pattern

In this analysis, we assume that each UE employs a directive antenna and communicates with its corresponding HAP base
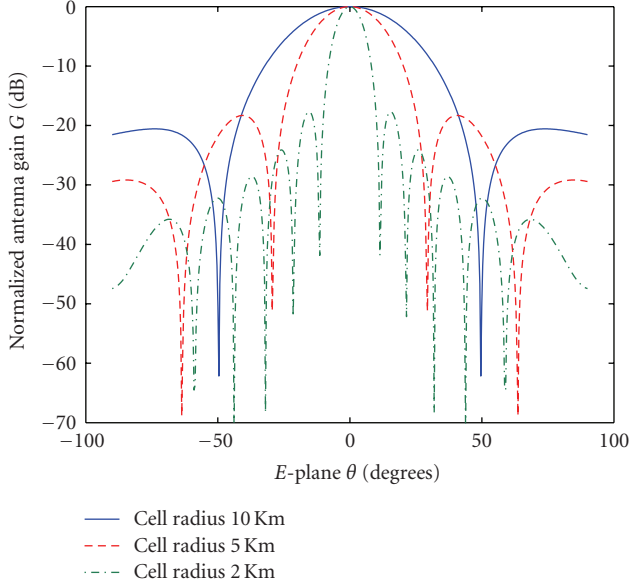
FIGURE 3: HAP base station antenna patterns for different cell radii.

TABLE 1: Antenna gains used in the simulation setup.

User equipment	Maximum antenna gain [dBi]
Mobile phone	0
Data terminal	2, 4, 12

gain from UE n to HAP m is then given by

$$g_{m,n}(\theta_m) = \left(l_{m,n}^{\text{FSL}} \cdot 10^{(L_f(\theta_m)/10)}\right)^{-1}. \tag{6}$$

2.5. WCDMA setup

The different service parameters used in this paper are collected from the 3GPP standard [29] and are summarised in Table 2. In order to account for the relative movement between the UE and the base stations, a fading propagation channel model based on (6) is simulated. This results in a block error rate (BLER) requirement of 1% for the 12.2 kbps voice service and a BLER of 10% for 64, 144, and 384 kbps data packet services, respectively.

3. INTERFERENCE ANALYSIS

Assuming that we have a setup of M different HAPs covering the same cell area and N users connected to each HAP, we can denote each UE position as $(x_{m,n}, y_{m,n})$, where $n = \{1, 2, \ldots, N\}$ and $m = \{1, 2, \ldots, M\}$. An example of a scenario setup with $N = 50$ and $M = 3$ is shown in Figure 2. The maximum power $p_{m,n}^{tx}$ that the user in location $(x_{m,n}, y_{m,n})$ is transmitting is dependent of the type of service used and can be obtained from Table 2. In WCDMA systems, power control is a powerful and essential method exerted in order to mitigate the near-far problem. The power received at base station (HAP) m from user n is

$$p_{m,n}^{rx}(\theta_m) = p_{m,n}^{tx} \cdot g_{m,n}(\theta_m), \tag{7}$$

where $g_{m,n}(\theta_m)$ is the total link gain, as defined in (6), between UE transmitter n and its own cell's BS receiver m. To be able to maintain a specific quality of service, we need to assert that we maintain a good enough signal-to-interference-plus-noise ratio (SINR) level. From Table 2, we can see the required E_b/N_0 values for different services, and we can express the required SINR, $\gamma_{m,n}$ for user n at HAP base station m as

$$\gamma_{m,n}^{\text{req}} = \frac{R}{W} \cdot \left(\frac{E_b}{N_0}\right)_{\text{req}}, \tag{8}$$

where R is the data rate of the service and W is the "chip rate" of the system. The required SINR can then be expressed as

$$\gamma_{m,n}^{\text{req}} = \frac{p_{m,n}^{rx}(\theta_m)}{I_{\text{tot}}}$$

$$= \frac{p_{m,n}^{tx}}{\sum_{m'=1}^{M} \sum_{\substack{n'=1 \\ n' \neq n}}^{N} p_{m',n'}^{tx} \cdot (g_{m',n'}(\theta_{m'})/g_{m,n}(\theta_m)) + p_w/g_{m,n}(\theta_m)},$$

$$m = \{1, 2, \ldots, M\}, \quad n = \{1, 2, \ldots, N\}, \tag{9a}$$

station. Using this assumption, we only need to set the desired maximum gain of the UE antenna we want to use, as shown Table 1. The antenna pattern of the directive antennas is calculated according to (1), but with a fixed maximum gain $G_{\max}$ instead of a fixed main beamwidth, the beamwidth is then $\varphi(G_{\max})$.

2.4. UE-HAP radio propagation channel model

In this paper, we use the combined empirical fading model (CEFM) together with the free space loss (FSL) model. CEFM combines the results of the empirical roadside shadowing (ERS) model [27] for low-elevation angles with the high-elevation angle results from [28] for the L and S bands. Using the FSL model, the path loss from UE n to HAP base station m is given by

$$l_{m,n}^{\text{FSL}} = \frac{(4 \cdot \pi \cdot d_{m,n})^2}{G_{m,n}^{rx} \cdot G_{m,n}^{tx} \cdot \lambda^2}, \tag{3}$$

where $d_{m,n}$ is the line of sight distance between the UE n and HAP m. The receiver $G_{m,n}^{rx}$ and transmitter $G_{m,n}^{tx}$ antenna gain patterns are calculated using (1) and (2). The carrier frequency f_c used in the simulation is 1.9 GHz which gives a wavelength λ of 0.1579 meters. The CEFM fading loss associated to HAP m is calculated as

$$L_f(\theta_m) = a \cdot \log_e(p) + b [\text{dB}], \tag{4}$$

where p is the percentile outage probability, and the data fitting coefficients a and b are calculated according to [27]

$$a = 0.002 \cdot \theta_m^2 - 0.15 \cdot \theta_m - 0.7 - 0.2 \cdot f_c,$$
$$b = 27.2 + 1.5 \cdot f_c - 0.33 \cdot \theta_m, \tag{5}$$

where θ_m is the elevation angle of HAP m. The total channel

Table 2: WCDMA service parameters employed in the simulation.

Parameters	Type of service			
	Voice	Data	Data	Data
Chip rate, W		3.84 Mcps		
Data rate, R	12 kbps	64 kbps	144 kbps	384 kbps
Required E_b/N_0	11.9 dB	6.2 dB	5.4 dB	5.8 dB
Maximum tx Power, $p_{m,n}^{tx}$	125 mW (21 dBm)	125 mW (21 dBm)	125 mW (21 dBm)	250 mW (24 dBm)
Voice activity	0.67	1	1	1

which can be formulated as

$$
\gamma_i^{\text{req}} = \frac{p_{m,n}^{tx}}{\sum_{\substack{k=1 \\ n' \neq n}}^{K} p_k^{tx} \cdot (g_k(\theta_{m'})/g_i(\theta_m)) + p_w/g_i(\theta_m)},
$$

$$
i = 1 + (n-1) + N(m-1) \in R^{K=M \cdot N},
$$

$$
m = \{1, 2, \ldots, M\}, \ n = \{1, 2, \ldots, N\},
$$

(9b)

with $K = M \cdot N$ as the total number of users in all cells and p_w is the additive white Gaussian noise (AWGN) at the receiver, where $\gamma_{m,n}^{\text{req}} \Rightarrow \gamma_i^{\text{req}}$, $g_{m',n'}(\theta_{m'}) \Rightarrow g_k(\theta_{m'})$, $g_{m,n}(\theta_m) \Rightarrow g_i(\theta_m)$, and $p_{m',n'}^{tx}(\theta_{m'}) \Rightarrow p_k^{tx}(\theta_{m'})$ are performed according to the index mapping rules in (9b). To solve for the transmitter power p_k^{tx} of each of the K individual UE simultaneously, (9b) can be reformulated into a matrix form as

$$
\mathbf{p}_{tx} = (\mathbf{I} - \mathbf{A})^{-1}\mathbf{b},
$$

(10)

where the calculated vector $\mathbf{p}_{tx}$ contains the necessary transmitter power level assigned to each of the K UE to fulfil the SINR requirement and where matrix $[\mathbf{A}]_{K \times K}$ and vector $[\mathbf{b}]_{K \times 1}$ are defined as

$$
[a_{ik}]_{K \times K} = \gamma_i^{\text{req}} \cdot \frac{gk(\theta_{m'})}{gi(\theta_m)} \quad \text{for } n' \neq n,
$$

$$
[a_{ik}] = 0 \quad \text{for } n' = n, \quad [b_i]_{K \times 1} = \gamma_i^{\text{req}} \cdot \frac{p_w}{gi(\theta_m)},
$$

$$
m = \{1, 2, \ldots, M\}, \ n = \{1, 2, \ldots, N\}, \quad (11)
$$

$$
i = 1 + (n-1) + N(m-1) \in R^{K=M \cdot N},
$$

$$
m' = \{1, 2, \ldots, M\}, \ n' = \{1, 2, \ldots, N\},
$$

$$
k = 1 + (n'=-1) + N(m'-1) \in R^{K=M \cdot N}.
$$

Using the $\mathbf{p}_{tx} = \mathbf{g} \odot \mathbf{p}_{tx}$, where $\odot$ denotes an elementwise multiplication and $\mathbf{g}$ is the total channel gain vector $[g_k]_{K \times 1}$ for all $k = \{1, 2, \ldots, K\}$ users, then all elements in the vector $\mathbf{p}_{tx}$ for each block that contain the UE of each of the M cells are balanced. The total cell interference can then be calculated as

$$
I_m^{\text{own}}(\theta_m) = \sum_{n=1}^{N} p_{m,n}^{rx}(\theta_m), \quad m = \{1, 2, \ldots, M\},
$$

$$
I_m^{\text{oth}}(\theta_m) = \sum_{\substack{m'=1 \\ m' \neq m}}^{M} \sum_{n=1}^{N} p_{m',n}^{rx}(\theta_{m'}) + p_w, \quad m = \{1, 2, \ldots, M\},
$$

(12)

where p_w is the thermal noise at the receiver, $I_m^{\text{own}}(\theta_m)$ is the interference from the UE within the own cell m, and $I_m^{\text{oth}}(\theta_m)$ is the interference from the UE in the $M-1$ other cells, where M is the total number of cells. We can now calculate $i_{\text{UL}}(\theta_m)$ which defines the other to own interference ratio for the uplink to HAP m and is given by

$$
i_{\text{UL}}(\theta_m) = \frac{I_m^{\text{oth}}(\theta_m)}{I_m^{\text{own}}(\theta_m)}.
$$

(13)

This is a performance measure of the simulated system capacity at a specific elevation angle θ_m towards the HAP (see Figure 1). If $i_{\text{UL}}(\theta_m)$ is between zero and one, there is possibility to have multiple HAP base stations covering the same coverage area. The actual number of users that can access the HAP base stations is also dependent of which data rate each user is using for transmission.

4. SIMULATION RESULTS

In this simulation, we assume that M HAPs are uniformly located along a circular boundary, with the centre of the circular boundary acting as the pointing direction of the HAPs base station antennas which simulate several overlapping cells; see Figure 1. The beamwidth of these base station antennas is determined by the radius of the cell coverage area (see Figures 1 and 2).

The aim of the simulation is to assess the effect of adding more HAPs on the system capacity. The distance d_m between the cell centre and the vertical projection of the HAP on the earth surface is denoted as "distance on the ground" and is varied from 0 to 70 km with a fixed cell position, as shown in Figure 4. The distance to the cell centre is also changing the elevation angle θ_m towards the HAP base station m as seen from the user. The cell radius has been set to 10 km and 30 km, and the HAP altitude is 20 km. Each HAP base station serves 100 users within each corresponding cell.

From Figure 5, it is clear that with the smaller cell radius (10 km), the worst case scenario will occur when all the HAPs
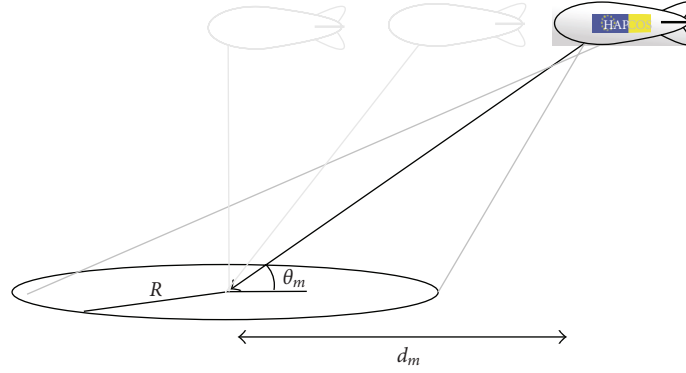
FIGURE 4: A plot illustrating the change of HAP position d_m to create different elevation angles θ_m.
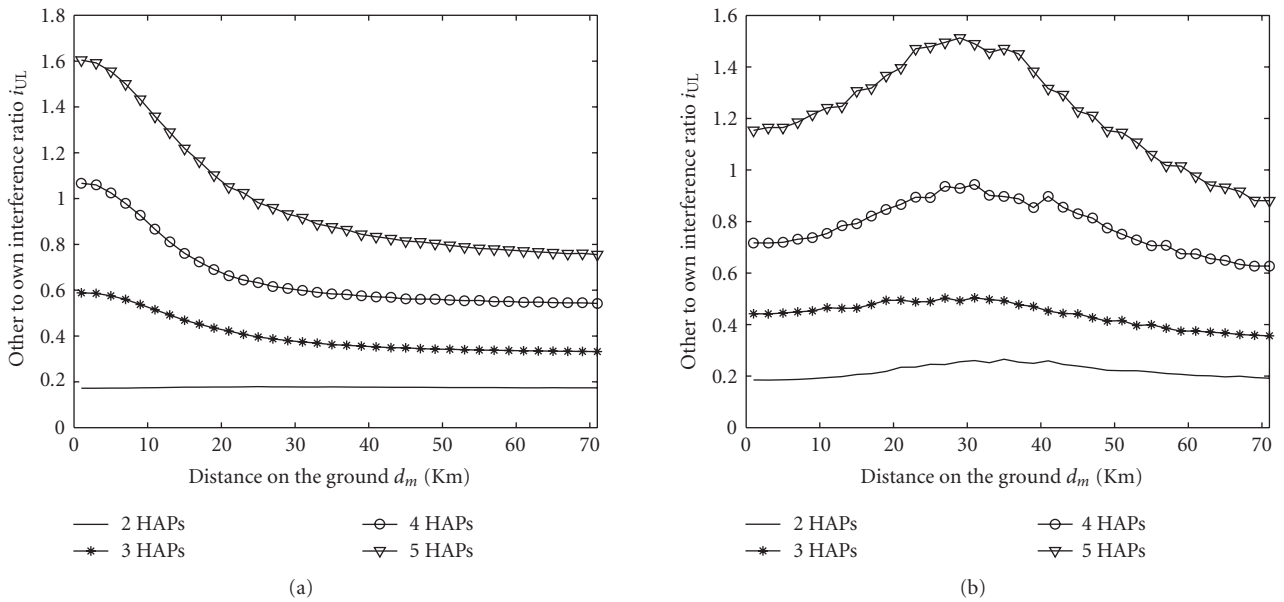

| (a) | (b) |

FIGURE 5: The performance of the voice service (12 kbps) from one HAP in combination with the data service (384 kbps) on the remaining HAPs for cell radius of 10 km (a) and 30 km (b). The distance on the ground d_m is varied from 0 to 70 km.

are stacked on top of each other at 90 degrees elevation angle from the cell centre (i.e., at a distance d_m on the ground of 0 km). In the larger cell radius case (30 m), the worst case scenario happens approximately at 30 km which is at the edge of the cell.

Comparing Figure 5(b) with the two diagrams in Figure 6, we can see that if we utilize a maximum allowed other-to-own interference ratio equal to one, then as the service data rate decreases, the number of possible HAP base stations covering the same area can increase from 2–4 HAPs (depending on the distance d_m between the cell centre and the vertical projection of the HAP on the ground) for the combined service (12 kbps and 384 kbps) to 6 HAPs with the same service (12 kbps on all HAPs). It is also clear from Figure 6 that the worst case distance (highest interference level) is at approximately 30 km, and consequently a worst case elevation angle of 34 degrees. This maximum interference level depends on the cell radius chosen for the HAP base station as shown in Figure 7. Simulations have shown that for cell radii larger than 10 km the maximum interference level will occur at the cell boundary.

5. CONCLUSIONS

In this paper, we have investigated the possibility of multiple HAP coverage of a common cell area in WCDMA systems and in particular we have studied the uplink. From these simulations, it is shown that as the service data rate decreases, the number of possible HAP base stations that can be deployed to cover the same geographical area increases. We have also shown that the worst case position of the HAPs is in the centre of the cell if the cell radius is small (<20 km) and at the cell boundary for large cells (>20 km). We can conclude that there is a possibility of deploying 3–5 HAPs covering the same cell area in response to an increase in traffic demands, depending on the type of service used.
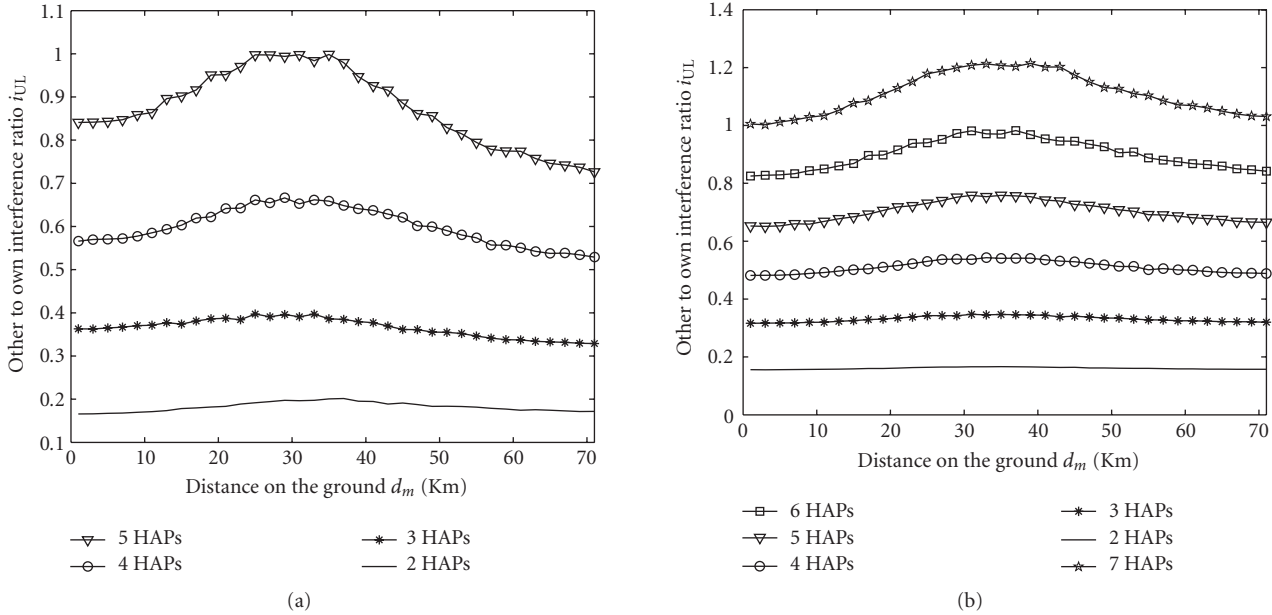
(a)

(b)

FIGURE 6: The other-to-own interference ratio obtained for a 30 km cell radius for (a) the performance of the voice service (12 kbps) from one HAP in combination with the data service (144 kbps) on the remaining HAPs and (b) the performance when we have voice services (12 kbps) on all HAPs. The distance on the ground d_m is varied from 0 to 70 km.
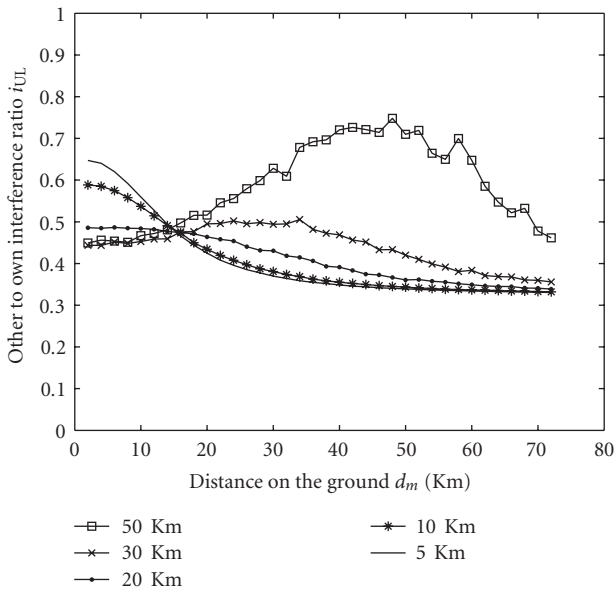

FIGURE 7: Illustrating the effect of HAP base station cell radius on interference levels. A system of 3 HAPs is utilized here and a voice service (12 kbps) from one HAP in combination with the data service (384 kbps) on the other HAPs. The distance on the ground d_m is varied from 0 to 70 km.

ACKNOWLEDGMENTS

REFERENCES

[1] R. Steele, "Guest editorial—an update on personal communications," *IEEE Communications Magazine*, vol. 30, no. 12, pp. 30–31, 1992.

[2] D. Grace, N. E. Daly, T. C. Tozer, A. G. Burr, and D. A. J. Pearce, "Providing multimedia communications services from high altitude platforms," *International Journal of Satellite Communications*, vol. 19, no. 6, pp. 559–580, 2001.

[3] G. M. Djuknic, J. Freidenfelds, and Y. Okunev, "Establishing wireless communications services via high-altitude aeronautical platforms: a concept whose time has come?" *IEEE Communications Magazine*, vol. 35, no. 9, pp. 128–135, 1997.

[4] M. J. Collela, J. N. Martin, and I. F. Akyildiz, "The HALO network^{TM}," *IEEE Communications Magazine*, vol. 38, no. 6, pp. 142–148, 2000.

[5] T. C. Tozer and D. Grace, "High-altitude platforms for wireless communications," *Electronics & Communication Engineering Journal*, vol. 13, no. 3, pp. 127–137, 2001.

[6] J. Thornton, D. Grace, C. Spillard, T. Konefal, and T. C. Tozer, "Broadband communications from a high-altitude platform: the European HeliNet programme," *Electronics & Communication Engineering Journal*, vol. 13, no. 3, pp. 138–144, 2001.

[7] D. Grace, M. H. Capstick, M. Mohorcic, J. Horwath, M. B. Pallavicini, and M. Fitch, "Integrating users into the wider broadband network via high altitude platforms," *IEEE Wireless Communications*, vol. 12, no. 5, pp. 98–105, 2005.

[8] R. Miura and M. Oodo, "Wireless communications system using stratospheric platforms," *Journal of the Communication Research Laboratory*, vol. 48, no. 4, pp. 33–48, 2001.

[9] J.-M. Park, B.-J. Ku, Y.-S. Kim, and D.-S. Ahn, "Technology development for wireless communications system using stratospheric platform in Korea," in *Proceedings of the 13th IEEE International Symposium on Personal, Indoor and Mobile Radio Communications (PIMRC '02)*, vol. 4, pp. 1577–1581, Lisbon, Portugal, September 2002.

[10] F. Dovis, R. Fantini, M. Mondin, and P. Savi, "Small-scale fading for high-altitude platform (HAP) propagation channels," *IEEE Journal on Selected Areas in Communications*, vol. 20, no. 3, pp. 641–647, 2002.

[11] Y. C. Foo, W. L. Lim, and R. Tafazolli, "Performance of high altitude platform station (HAPS) in delivery of IMT-2000 W-CDMA," in *Proceedings of the Stratospheric Platform Systems Workshop*, Tokyo, Japan, September 2000.

[12] E. Falletti, M. Mondin, F. Dovis, and D. Grace, "Integration of a HAP within a terrestrial UMTS network: interference analysis and cell dimensioning," *Wireless Personal Communications*, vol. 24, no. 2, pp. 291–325, 2003.

[13] S. Masumura and M. Nakagawa, "Joint system of terrestrial and high altitude platform station (HAPS) cellular for W-CDMA mobile communications," *IEICE Transactions on Communications*, vol. E85-B, no. 10, pp. 2051–2058, 2002.

[14] M. A. Vázquez-Castro, D. Belay-Zelek, and A. Curieses-Guerrero, "Availability of systems based on satellites with spatial diversity and HAPS," *Electronics Letters*, vol. 38, no. 6, pp. 286–288, 2002.

[15] Recommendation ITU-R M.1456, "Minimum performance characteristics and operational conditions for high altitude platform stations providing IMT-2000 in the bands 1885–1980 MHz, 2010–2025 MHz and 2110–2170 MHz in the regions 1 and 3 and 1885–1980 MHz and 2110–2160 MHz in region 2," International Telecommunications Union, 2000.

[16] Recommendation ITU-R F.1500, "Preferred characteristics of systems in the fixed service using high-altitude platform stations operating in the bands 47.2–47.5 GHz and 47.9–48.2 GHz," International Telecommunications Union, 2000.

[17] M. Oodo, R. Miura, T. Hori, T. Morisaki, K. Kashiki, and M. Suzuki, "Sharing and compatibility study between fixed service using high altitude platform stations (HAPS) and other services in the 31/28 GHz bands," *Wireless Personal Communications*, vol. 23, no. 1, pp. 3–14, 2002.

[18] B. El-Jabu and R. Steele, "Cellular communications using aerial platforms," *IEEE Transactions on Vehicular Technology*, vol. 50, no. 3, pp. 686–700, 2001.

[19] J. Thornton, D. Grace, M. H. Capstick, and T. C. Tozer, "Optimizing an array of antennas for cellular coverage from a high altitude platform," *IEEE Transactions on Wireless Communications*, vol. 2, no. 3, pp. 484–492, 2003.

[20] J. Thornton and D. Grace, "Effect of lateral displacement of a high-altitude platform on cellular interference and handover," *IEEE Transactions on Wireless Communications*, vol. 4, no. 4, pp. 1483–1490, 2005.

[21] D. Grace, C. Spillard, J. Thornton, and T. C. Tozer, "Channel assignment strategies for a high altitude platform spot-beam architecture," in *Proceedings of the 13th IEEE International Symposium on Personal, Indoor and Mobile Radio Communications (PIMRC '02)*, vol. 4, pp. 1586–1590, Lisbon, Portugal, September 2002.

[22] D. Grace, J. Thornton, G. Chen, G. P. White, and T. C. Tozer, "Improving the system capacity of broadband services using multiple high-altitude platforms," *IEEE Transactions on Wireless Communications*, vol. 4, no. 2, pp. 700–709, 2005.

[23] G. Chen, D. Grace, and T. C. Tozer, "Performance of multiple high altitude platforms using directive HAP and user antennas," *Wireless Personal Communications*, vol. 32, no. 3-4, pp. 275–299, 2005.

[24] Y. Liu, D. Grace, and P. D. Mitchell, "Effective system spectral efficiency applied to a multiple high-altitude platform system," *IEE Proceedings: Communications*, vol. 152, no. 6, pp. 855–860, 2005.

[25] D. Grace and P. Likitthanasate, "A business modelling approach for broadband services from high altitude platforms," in *Proceedings of the International Conference on Telecommunications (ICT '06)*, Madeira, Portugal, May 2006.

[26] C. A. Balanis, *Antenna Theory: Analysis and Design*, chapter 6, John Wiley & Sons, New York, NY, USA, 1997.

[27] J. Goldhirsch and W. J. Vogel, "Propagation effects for land mobile satellite systems: overview of experimental and modeling results," NASA Reference Publication 1274, February 1992.

[28] M. A. N. Parks, G. Butt, B. G. Evans, and M. Richharia, "Results of multiband (L, S, Ku band) propagation measurements and model for high elevation angle land mobile satellite channel," in *Proceedings of the 17th NASA Propagation Experimenters Meeting (NAPEX 17) and the Advanced Communications Technology Satellite (ACTS) Propagation Studies Miniworkshop*, pp. 193–202, Pasadena, Calif, USA, June 1993.

[29] "Base Station (BS) radio transmission and reception," 3GPP TS 25.104, http://www.3gpp.org/specs/specs.htm.